AFCRL-67-0475
AUGUST 1967
ENVIRONMENTAL RESEARCH PAPERS, NO. 273

AIR FORCE CAMBRIDGE RESEARCH LABORATORIES
L. G. HANSCOM FIELD, BEDFORD, MASSACHUSETTS

Shear Strength of Twelve Grossly Deformed Metals at High Pressures and Temperatures

R. E. RIECKER
L. C. TOWLE
T. P. ROONEY

This work was supported by the Advanced Research Projects Agency under ARPA Project 8671

OFFICE OF AEROSPACE RESEARCH
United States Air Force

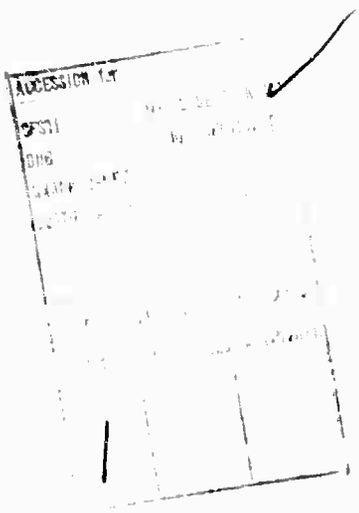

AFCRL-67-0475
AUGUST 1967
ENVIRONMENTAL RESEARCH PAPERS, NO. 273

TERRESTRIAL SCIENCES LABORATORY PROJECT 7639

AIR FORCE CAMBRIDGE RESEARCH LABORATORIES
L. G. HANSCOM FIELD, BEDFORD, MASSACHUSETTS

Shear Strength of Twelve Grossly Deformed Metals at High Pressures and Temperatures

R. E. RIECKER
L. C. TOWLE*
T. P. ROONEY

*U.S. Naval Research Laboratory, Washington, D.C.

This work was supported by the Advanced Research Projects Agency under ARPA Project 8671

OFFICE OF AEROSPACE RESEARCH
United States Air Force

Abstract

The shear strength of grossly deformed tungsten, germanium, nickel, beryllium, uranium, copper, gold, silver, aluminum, magnesium, bismuth, and tin was measured in an opposed anvil shear apparatus at pressures up to 150 kb at 27°C, and for gold, silver, and copper to a maximum of 900°C. The shear data agree with independent strength measurements at low pressures, but differ significantly from high-pressure shear-strength measurements made by other investigators. The data on the noble metals also fit a simple empirical formula relating the temperature and pressure dependence of the shear strength.

BLANK PAGE

Contents

Illustrations

Illustrations

Tables

Shear Strength of Twelve Grossly Deformed Metals at High Pressures and Temperatures

1. INTRODUCTION

The shear strength of pure, single-phase metals depends principally on temperature, pressure, dislocation density, and strain-rate. In general, dislocation density is not an independent variable, since it depends on the detailed history of the material. However, when a metal deforms continuously at a constant strain-rate, temperature, and pressure, the dislocation density approaches a saturation value appropriate to the dynamic equilibrium conditions that prevail. Under these circumstances one would hope that the shear strength would depend on temperature, pressure, and strain-rate through some relatively simple relationship. The shear strength of a metal in the grossly deformed state represents the maximum that can be obtained by workhardening. Thus the study of grossly deformed metals is of both theoretical and practical interest.

The shear strength of pure tungsten, germanium, nickel, beryllium, uranium, copper, gold, silver, aluminum, magnesium, bismuth, and tin was measured in an opposed anvil shear press from 10 kb to a maximum of 150 kb at 27°C, and high-temperature tests to a maximum of 900°C were made on the noble elements copper, silver, and gold. The results exhibit internal consistency and agree with independent measurements made at low pressures. The new data on the noble metals also fit a recently reported emperical relationship giving the temperature and pressure dependence of the shear strength of grossly

(Received for publication 14 August 1967)

deformed materials (Towle, 1967). The present results differ significantly from earlier room-temperature measurements by Bridgman (1935, 1937) in the limited pressure range to 50 kb and by Vereshchagin and Shapochkin (1960) to 150 kb.

2. EXPERIMENTAL

The shear press used in the tests reported herein is similar to that employed originally by Bridgman (1935, 1937) and to a more recent design of Vereshchagin et al. (1960). We described the apparatus in detail elsewhere (Riecker, 1964a; 1964b). The essential features include a 0.25-in.-diam, 0.010-in.-thick sample wafer that is compressed by a hydraulic ram between a pair of tungsten carbide anvils having 0.25-in.-diam, flat circular faces. The upper anvil is rotated at constant speed by a variable-speed motor through a gear train. A lever arm prevents rotation of the lower anvil and is anchored to the press frame through a strain-gage load cell. High-temperature operation is achieved by external induction heating of the anvils.

The directly observed physical quantities include: anvil temperature, T; normal load applied to the anvils, N; rotation rate of the upper anvil, R; and the force applied through the load cell to prevent rotation of the lower anvil, F. An infrared pyrometer records the temperature of the sample; it is calibrated with chromel-alumel thermocouples placed in exact duplicates of the anvils. Observed temperatures are accurate within ± 2 percent. Pressure applied to the sample is calculated from the force per unit sample area. Reproducibility approaches ± 3 percent, as determined using bismuth I-II and thallium II-III phase transitions to calibrate the press. A Variac motor-speed control calibrated under loads to 200 kb determines the anvil rotation rate. A strip-chart recorder monitors the load cell output force, and when multiplied by the lever arm length, L, gives a continuous record of the torque M, required to prevent rotation of the lower anvil.

Measurements were made on samples having purities of 99.995 percent or better obtained from the Lawrence Radiation Laboratory. Each metal, except for Bi and SN, was cross-rolled to a thickness of 0.010 in. and then annealed for 1 to 2 hr at 500°C. We obtained all data at a constant rotation-rate of 10 revolutions per hour^{-1}, which corresponds to an average strain-rate of about 10^{-1} sec^{-1}. The metals were sheared following application of pressure and temperature. A fresh sample was used for each datum point, except where noted. This procedure prevented frequent anvil-to-anvil contact at the sample periphery which would have led to erroneous results.

In previous shear measurements on silicate insulating materials (Riecker and Rooney, 1965; 1966), we monitored the electrical resistance between anvils as a means of detecting anvil-to-anvil contact. After shearing a sample at one

pressure, anvil-to-anvil contact usually developed if we attempted to shear the sample again at a higher pressure. Contact frequently caused a 2- or 3-fold increase in shearing torque. Consequently, we used fresh samples for each datum point. Since resistance monitoring is not possible with metallic samples, the torque-time records were carefully inspected to verify that anvil-to-anvil contact had not occurred. In spite of the use of a fresh sample in each test, a few spurious results attributable to contact were discovered and rejected.

A typical torque-time curve is shown schematically in Figure 1. The figure shows an initial transient state that persists through an angle of about 10 deg, after which a steady state develops. During the transient period the sample reaches an equilibrium thickness, workhardens, and develops some preferred orientation. Only the steady-state torque value is used in the shear-strength calculations.

Evidence supporting the behavior of the grossly deformed wafers during the transient period is provided by observations made on microhardness, thickness profile, and metallographic textures of sheared wafers. The typical thickness of deformed copper wafers varies from 0.010 in. in virgin metal to 0.0010 in. (Figure 2) at the wafer periphery (Figure 3), and 0.003 in. at the center (Figure 4). Virgin copper grain size averages about 0.001 in. in diameter, but drops to less than 0.0001 in. in deformed regions. Some grains show extreme flattening in directions normal to the applied load (Figure 3).

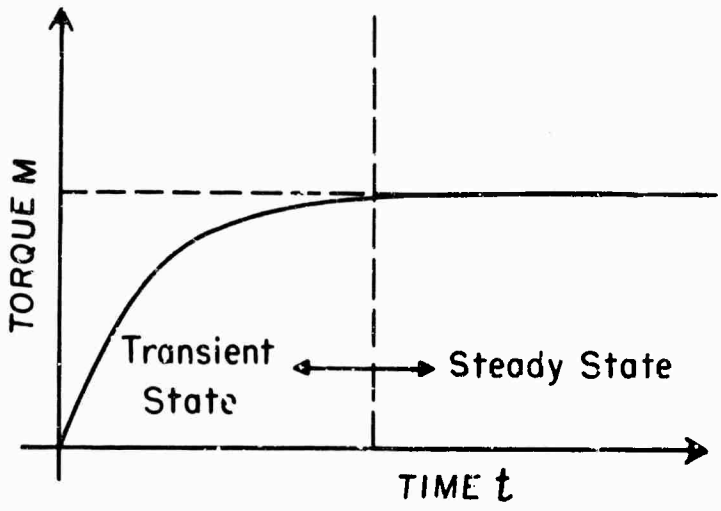

Figure 1. Torque-Time Curve Showing Schematically That a Significant Transient State Always Exists. Workhardening occurs during this period regardless whether the final steady-state is one of surficial slip or internal shear

Figure 2. Metallographic Cross Section Through Deformed Wafer Showing Undeformed Segment. Note thickness of specimen and large grain size. Axis of normal pressure located vertically. Scale line is 0.05 mm

Figure 3. Metallographic Cross Section Through Deformed Wafer Showing Most Severely Deformed Periphery. Sample was originally same size as that in Figure 2. Note grain distortion and comminution. Normal pressure axis located vertically. Scale line is 0.05 mm

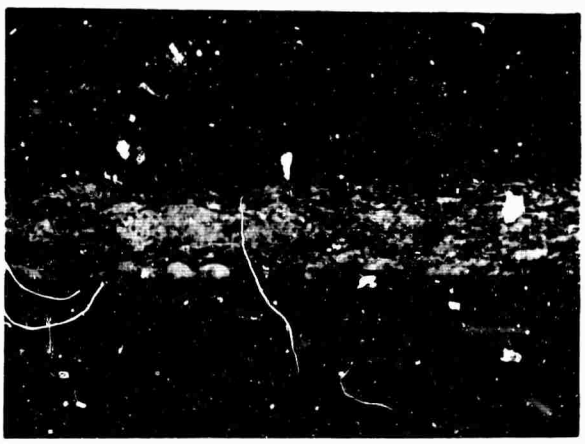

Figure 4. Metallographic Cross Section Through Deformed Wafer at Center. Normal pressure axis located vertically. Scale is 0.05 mm

The severe distortional changes and comminution in grains graphically illustrate the magnitude of the induced strain. Knoop microhardness tests made along diametral cross sections also quantitatively show the degree of strain hardening that develops during gross shear. Virgin copper gives a diamond pyramidal number of 63. Hardness at the periphery of deformed wafers is 100 or more, while hardness at the wafer center ranges from 80 to 90. These measurements show that the metal wafers receive gross strain, and that the metal strainhardens in response to gross shear.

The frictional stress at the sample-anvil interface is given by μP where μ is the coefficient of friction and P is normal pressure. At low pressures $\mu P < S$, where S is the shear strength of the sample, and therefore surficial slippage must occur. However, μP normally increases with pressure faster than S, and eventually a pressure is reached at which the deformation mechanism switches to internal shear. It is only at high pressures that useful data are obtained with this apparatus.

Onset of anvil-to-anvil contact in the slip regime has little effect on the torque, since the friction coefficient is not greatly altered. If contact occurs in the shearing regime where $\mu P > S$, then torque rises sharply. However, consistent anvil contact produces normal looking torque-time curves, even though the steady-state torque may be erroneously large. As a consequence, when a single sample is repeatedly sheared through the entire pressure range, as was done by Bridgman and by Vereshchagin and Shapochkin, anvil-to-anvil contact can easily escape unnoticed. Hence, some of their measurements are open to serious question.

3. THEORETICAL MODEL

The analysis of shear measurements is based on a model originally proposed by Bridgman (1935, 1937). In order to avoid misinterpretations, we indicate the major approximations made in deriving the calculated shear strength from the observed quantities.

The relation of rotation angle to applied strain is obtained by considering the torsion of a short circular cylinder. Shear strain γ relates to the angle of rotation θ by the expression

$$\gamma = \frac{r}{h}\theta \qquad (1)$$

where h is the height of the cylinder and r is the radius at which the strain is calculated. Strain increases linearly from zero at the symmetry axis to a maximum at the periphery. For the sample geometry employed here, $\gamma \sim 12.5\theta$ at the periphery, that is, extremely large strains are applied by small angels of rotation.

The torque required to prevent rotation of the lower anvil is given by $M = L \times F$. This restraining moment can also be expressed by the integral

$$M = \int_0^a \tau \times r \times 2\pi\, r dr \tag{2}$$

where τ is the shear stress at the distance r from the axis of rotation, and $2\pi\, r dr$ is an annular element of area in the sample wafer. The value assumed by the shear stress τ depends on the deformation mechanism which prevails. The mechanism can be either surficial slip at the sample-anvil interfaces, or internal shear within the sample. The mechanism requiring the lower activation stress prevails.

In the low pressure surficial slip regime, $\tau = \mu P$, and the restraining torque is

$$M = \frac{2\pi a^3}{3}\, \mu P \tag{3}$$

where a is the anvil radius. In the high pressure regime, $\tau = S(T, P)$, where the possible dependence of shear strength on temperature and pressure is recognized. For gross deformation, S will not depend on strain. Furthermore, Bridgman (1937) showed that the shear strength of copper and high-melting-point materials varies only moderately with strain-rate. Thus, we also assume that S is independent of $\dot{\gamma}$ in what follows.

In principle, hydrostatic pressure should increase the strength of materials. However, the observed increases normally are quite small. Conventional engineering practice assumes that shear strength is independent of pressure. We will assume that shear strength can be expanded in a Taylor's Series expansion on the pressure variable and retain only the linear term. Thus,

$$S = S_1 + \alpha P \tag{4}$$

where S_1 is the shear strength at atmospheric pressure. The shearing torque then becomes

$$M = \frac{2\pi a^3}{3}(S_1 + \alpha P). \tag{5}$$

It is common practice to divide the observed restraining torques by the numerical factor $2\pi a^3/3$ and call the result the shear strength. The data are then plotted as shown by the heavy curve in Figure 5. Figure 5 approximates the idealized curves at very low and very high pressures where Eqs. (3) and (5) apply. The idealized curves intersect at the pressure P_k for which $\mu P = S$, that is,

$$P_k = \frac{S}{\mu - \alpha} \quad . \tag{6}$$

When we consider the effects of pressure gradients in the sample, the transition from surficial slip to internal shear occurs smoothly, as indicated by the knee in the heavy curve. Therefore, the data obtained at low pressures, to the left of the knee, bear no immediate relation to the shear strength of the material.

Figure 6 shows schematically the pressure distribution across the anvil radius. It varies gradually over the central portion of the sample and changes rapidly near the periphery. Figure 6 reveals that internal shear occurs after some minimum threshold pressure develops at the center of the sample. With further increases in load, the boundary between shear and slip regimes, r_e, increases rather rapidly until it falls between r_e and a. This boundary then moves outward very slowly with increased pressure. In principle, slip always occurs in a small annular region around the periphery regardless of the pressure applied. This nonuniform pressure distribution leads to a smooth transition from the slip to internal shear. The effects of incorporating a realistic pressure gradient into the derivation given above were considered in detail elsewhere by Towle and Riecker (1966). For large loads where $r_e > r_e$ and the bulk of the sample shears internally, the error incurred by neglecting the pressure gradient is typically less than 15 percent.

Three characteristics of shear measurements in opposed anvil devices should be emphasized: (1) valid shear-strength data can be obtained only above a threshold pressure that may be quite high for materials that are intrinsically strong or that workharden extensively. This threshold can be estimated from Eq. (6) and is typically in the range from 10 to 50 kb; (2) useful data are obtained only in the steady-state condition after the sample has been grossly deformed; (3) sample deformation and workhardening occur under all pressure conditions in metals, as evidenced by the transient portion of the torque-time curves, although surficial slip dominates the final behavior at low pressures.

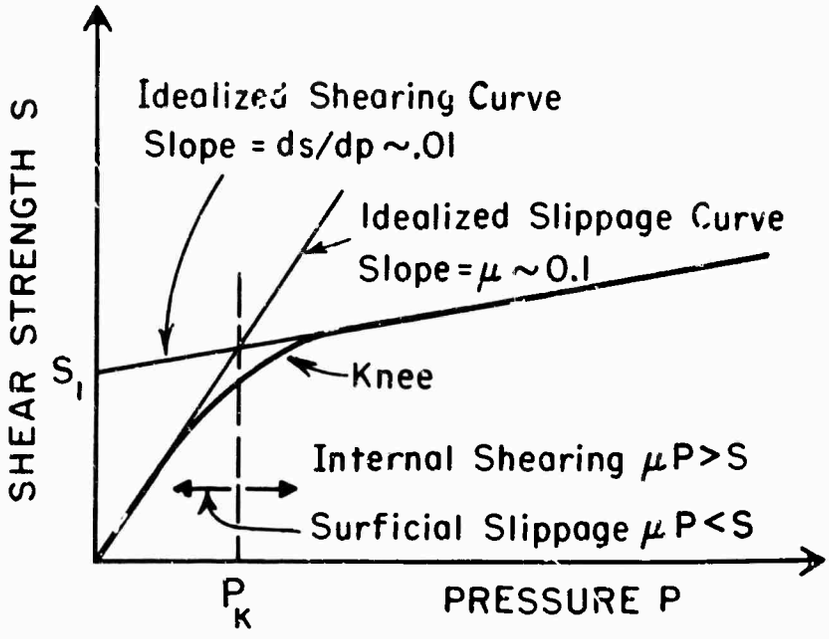

Figure 5. Schematic Showing Relation Between Observed Data and Idealized Modes of Behavior, Internal Shear, and Surficial Slip

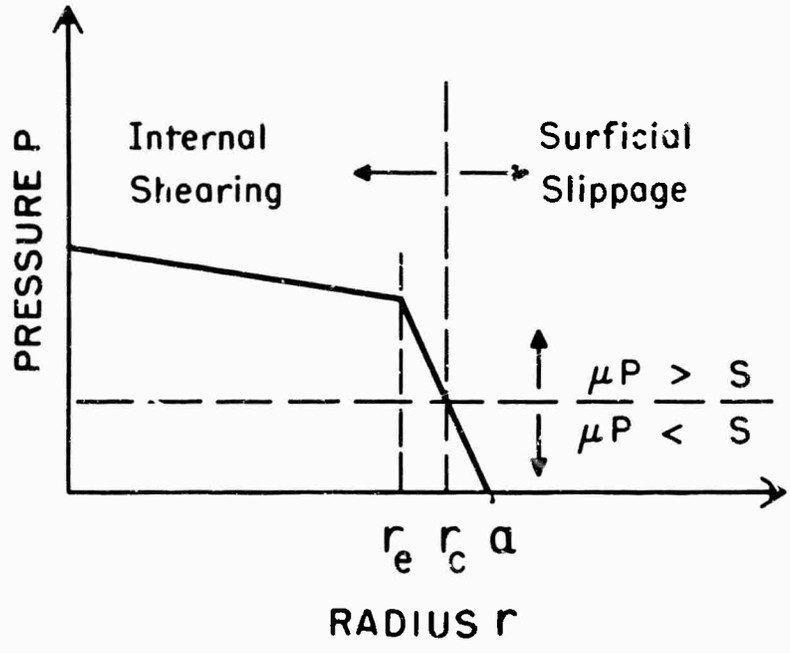

Figure 6. Pressure Distribution vs Radial Position of Deformed Wafer. Surficial slip always occurs at periphery of wafer where frictional stress drops below the shear strength of the sample

4. RESULTS

Figures 7, 8, and 9 show the shear-strength normal-pressure curves obtained at room temperature for tungsten, uranium, nickel, beryllium, copper, silver, gold, aluminum, magnesium, bismuth, and tin. Tables 1 through 11 give the test conditions and shear-strength values observed Some elements were not sheared to 150 kb due to excessive anvil failure. The curves in Figures 7, 8, and 9 clearly show the qualitative form anticipated by the theoretical model indicated in Figure 5.

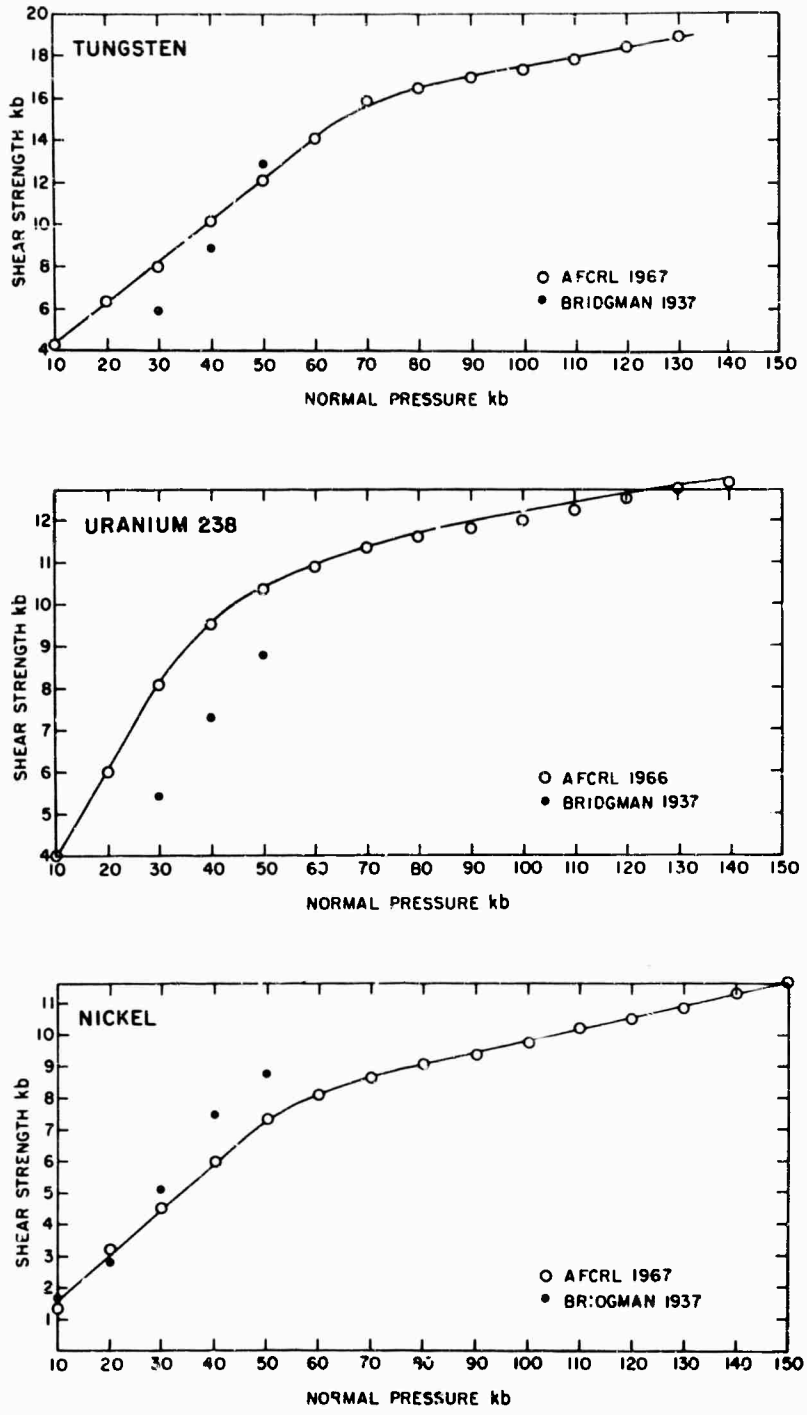

Figure 7. Shear Curves for Tungsten, Uranium, and Nickel at 27°C and a Strain Rate of 10^{-1} sec $^{-1}$. Test conditions given in Tables 1, 2, and 3

Table 1. Test Conditions for Tungsten

Tungsten 27°C			
Test Number	Normal Pressure (kb)	Total Revolutions (at 9.6 rph)	Shear Strength (kb)
W1-1	9.95	1.12	4.3
W1-5	49.74	2.24	12.1
W1-6	9.95	1.92	4.3
W1-7	19.90	1.12	6.3
W1-8	29.85	1.76	8.0
W1-9	39.79	1.44	10.2
W1-11	59.69	1.12	14.1
W1-12	69.64	0.48	15.8
W1-13	79.59	0.88	16.4
W1-14	89.54	0.64	16.9
W1-15	99.49	0.80	17.4
W1-16	109.44	0.64	17.8
W1-17	119.39	0.48	18.45
W1-18	129.33	0.40	18.9

Other Data					
Bridgman (1937)					
Normal Pressure (kb)	10	20	30	40	50
Shear Strength (kb)	1.1	3.1	5.8	8.9	12.8

Table 2. Test Conditions for Uranium

Uranium 238 27°C			
Test Number	Normal Pressure (kb)	Total Revolutions (at 9.6 rph)	Shear Strength (kb)
Ur1-1	9.95	0.80	4.0
Ur1-2	19.90	0.64	6.0
Ur1-3	29.85	0.48	8.1
Ur1-4	39.79	0.64	9.5
Ur1-5	49.74	0.64	10.4
Ur1-8	59.69	0.96	10.9
Ur1-9	69.64	0.64	11.4
Ur1-10	79.59	0.32	11.6
Ur1-11	89.54	0.40	11.8
Ur1-12	99.49	0.40	12.0
Ur1-13	109.44	0.32	12.2
Ur1-14	119.39	0.32	12.5
Ur1-15	129.33	0.40	12.7
Ur1-16	139.28	0.64	12.9

Other Data					
Bridgman (1937)					
Normal Pressure (kb)	10	20	30	40	50
Shear Strength (kb)	0.7	2.8	5.4	7.3	8.8

Table 3. Test Conditions for Nickel

Nickel 27°C			
Test Number	Normal Pressure (kb)	Total Revolutions (at 9.6 rph)	Shear Strength (kb)
Ni1-3	29.85	0.80	4.55
Ni1-4	9.95	0.64	1.8
Ni1-5	19.90	0.95	3.2
Ni1-6	39.79	1.12	6.0
Ni1-7	49.74	0.80	7.35
Ni1-8	59.69	0.96	8.1
Ni1-9	69.64	0.80	8.6
Ni1-10	79.59	0.80	9.1
Ni1-11	89.54	0.56	9.4
Ni1-12	99.49	0.48	9.8
Ni1-13	109.44	0.56	10.2
Ni1-14	119.39	0.48	10.5
Ni1-15	129.33	0.48	10.9
Ni1-18	139.28	0.48	11.3
Ni1-17	149.23	0.48	11.7

Other Data					
Bridgman (1937)					
Normal Pressure (kb)	10	20	30	40	50
Shear Strength (kb)	1.0	2.3	5.2	7.5	8.7

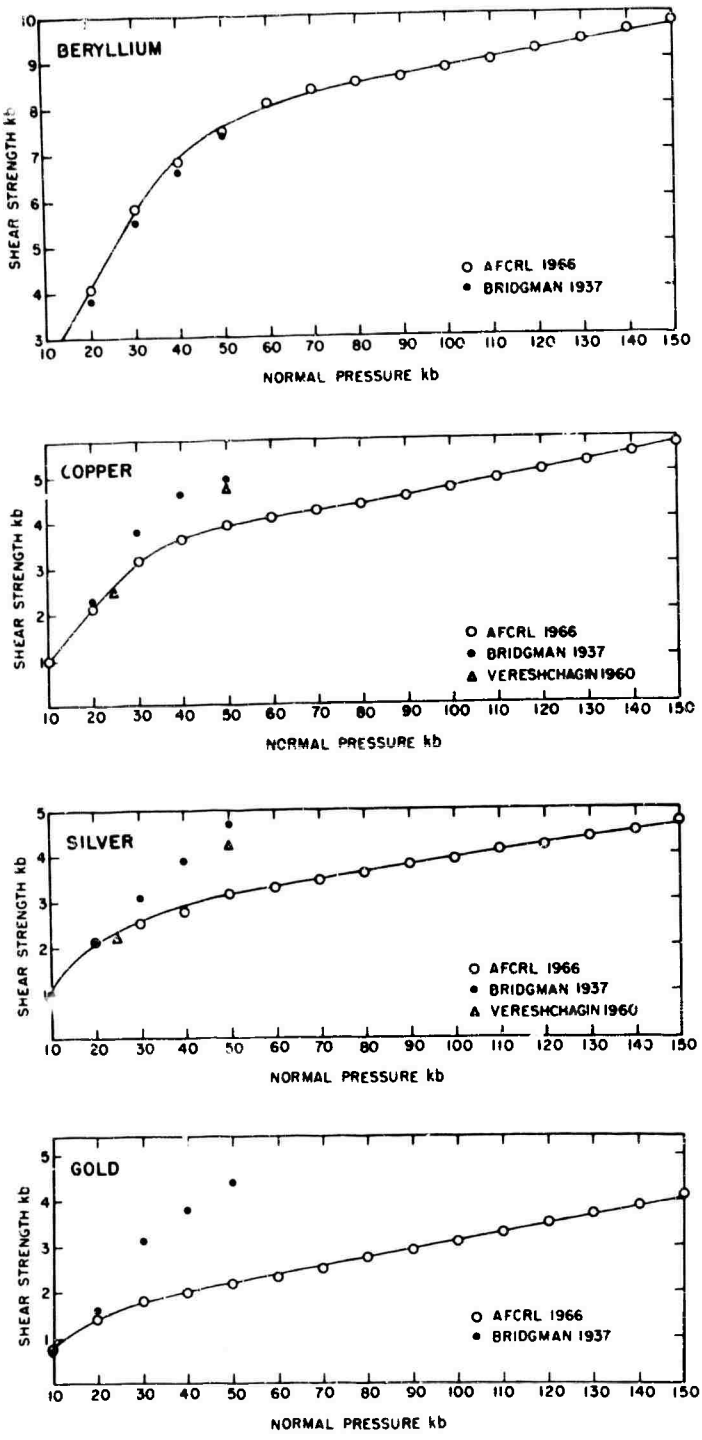

Figure 8. Shear Curves for Beryllium, Copper, Silver, and Gold at 27°C and a Strain Rate of 10^{-1} sec^{-1}. Test conditions given in Tables 4 through 7

Table 4. Test Conditions for Beryllium

Beryllium 27°C			
Test Number	Normal Pressure (kb)	Total Revolutions (at 9.6 rph)	Shear Strength (kb)
Bel-1	9.95	0.80	2.3
Bel-2	19.90	0.64	4.0
Bel-3	29.85	0.64	5.8
Bel-4	39.79	0.48	6.8
Bel-5	49.74	0.48	7.5
Bel-6	59.69	0.48	8.1
Bel-7	69.64	0.48	8.3
Bel-8	79.59	0.56	8.5
Bel-9	89.54	0.48	8.6
Bel-10	99.49	0.48	8.8
Bel-11	109.44	0.48	9.0
Bel-12	119.39	0.48	9.2
Bel-13	129.33	0.48	9.4
Bel-14	139.28	0.32	9.6
Bel-15	149.23	0.48	9.8
Other Data			
Bridgman (1937)			
Normal Pressure (kb)	10	20	30	40	50
Shear Strength (kb)	1.6	3.8	5.5	6.6	7.4

Table 5. Test Conditions for Copper

Copper 27°C			
Test Number	Normal Pressure (kb)	Total Revolutions (at 9.6 rph)	Shear Strength (kb)
Cul-1	9.95	0.48	[illegible]
Cul-2	19.90	0.48	[illegible].1
Cul-3	29.85	1.12	3.2
Cul-4	29.85	0.96	3.3
Cul-6	49.74	0.64	3.9
Cul-7	59.69	0.96	4.1
Cul-8	39.79	0.73	3.6
Cul-9	69.64	0.51	4.2
Cul-10	79.59	0.48	4.4
Cul-11	89.54	0.67	4.5
Cul-12	99.49	0.40	4.7
Cul-14	119.39	0.88	5.1
Cul-15	109.44	0.48	4.9
Cul-17	129.33	0.64	5.3
Cul-18	139.28	0.40	5.4
Cul-19	149.23	0.96	5.[illegible]
Cul-21	39.79	1.12	3.8
Other Data			
Bridgman (1937)			
Normal Pressure (kb)	10	20	30	40	50
Shear Strength (kb)	1.0	2.3	3.8	4.6	4.9
Vereshchagin (1960)			
Normal Pressure (kb)	25	50	100		
Shear Strength (kb)	2.5	4.7	11.3		

Table 6. Test Conditions for Silver

Silver 27°C			
Test Number	Normal Pressure (kb)	Total Revolutions (at 9.6 rph)	Shear Strength (kb)
Agl-1	9.85	0.80	0.9
Agl-2	19.90	0.96	2.2
Agl-3	29.85	1.60	2.5
Agl-4	39.78	1.28	2.8
Agl-5	49.74	1.28	3.2
Agl-6	58.68	0.96	3.3
Agl-7	69.64	0.88	3.5
Agl-8	79.59	0.64	3.6
Agl-9	88.54	0.48	3.8
Agl-10	89.48	0.48	3.8
Agl-11	109.44	0.48	4.1
Agl-12	119.39	0.58	4.2
Agl-13	129.33	0.46	4.4
Agl-14	138.28	0.32	4.5
Agl-15	148.23	0.48	4.7
Other Data			
Bridgman (1837)			
Normal Pressure (kb)	10	20	30	40	50
Shear Strength (kb)	1.0	2.1	3.1	3.8	4.7
Vereshchagin (1960)			
Normal Pressure (kb)	25	50	100	150	
Shear Strength (kb)	2.2	4.2	8.1	10.4	

Table 7. Test Conditions for Gold

Gold 27°C			
Test Number	Normal Pressure (kb)	Total Revolutions (at 9.6 rph)	Shear Strength (kb)
Aul-1	9.95	0.80	[illegible]5
Aul-2	19.90	1.28	1.4
Aul-3	29.65	0.96	1.7
Aul-4	39.79	0.80	1.9
Aul-5	49.74	0.48	2.1
Aul-6	59.69	0.48	2.3
Aul-7	69.64	0.48	2.5
Aul-8	79.59	0.32	2.7
Aul-9	89.54	0.32	2.9
Aul-10	99.49	0.48	3.1
Aul-11	109.44	0.32	3.3
Aul-12	119.39	0.40	3.5
Aul-13	129.33	0.32	3.7
Aul-14	139.28	0.32	3.9
Aul-15	149.23	0.48	4.1
Other Data			
Bridgman (1937)			
Normal Pressure (kb)	10	20	30	40	50
Shear Strength (kb)	0.7	1.6	3.1	3.8	4.4

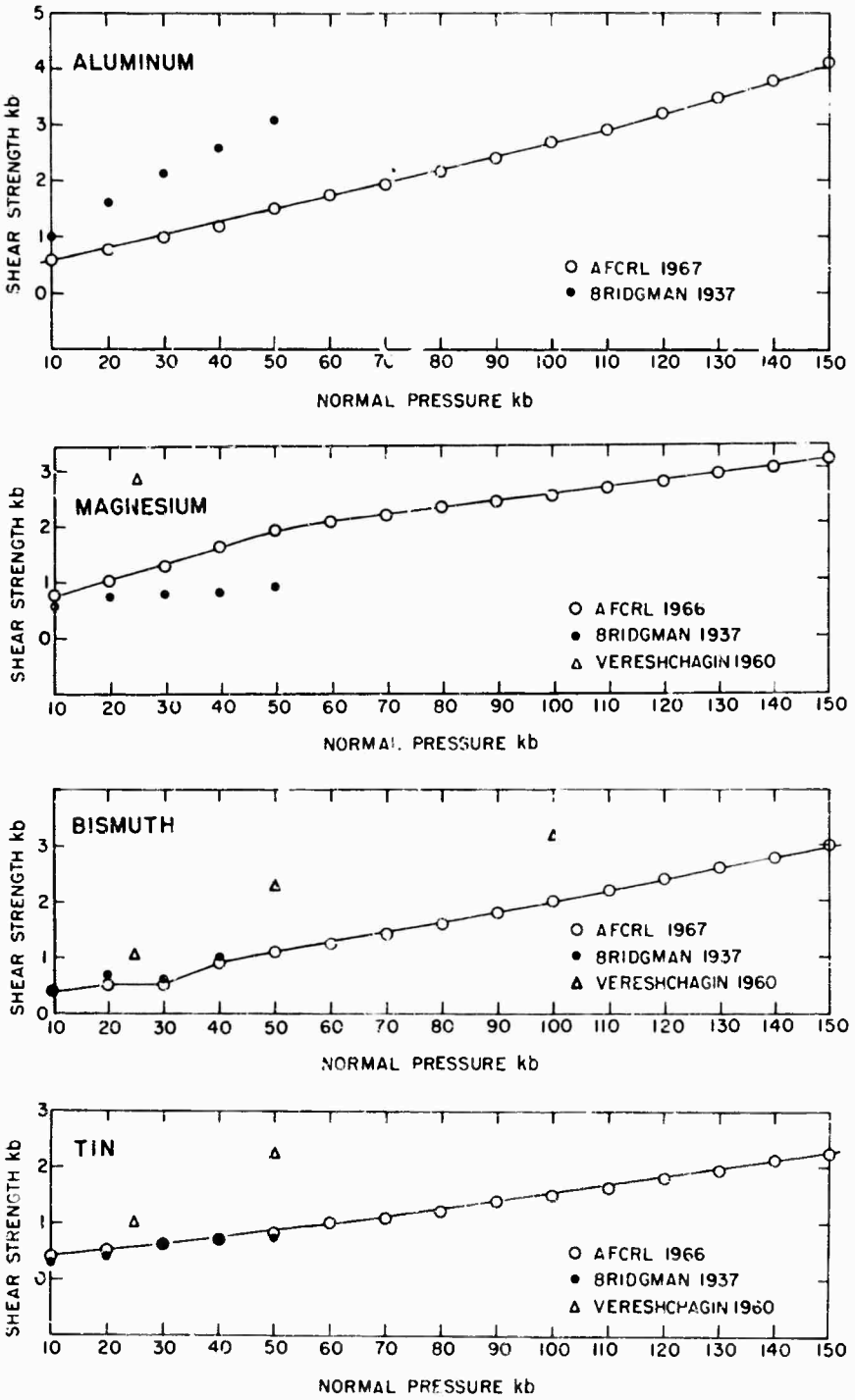

Figure 9. Shear Curves for Aluminum, Magnesium, Bismuth, and Tin at 27°C and a Strain Rate of 10^{-1} sec^{-1}. Test conditions given in Tables 8 through 11

Table 8. Test Conditions for Alluminum

Aluminum 27°C			
Test Number	Normal Pressure (kb)	Total Revolutions (at 9.6 rph)	Shear Strength (kb)
Al 1-1	9.95	0.80	0.6
Al 1-2	19.90	0.96	0.8
Al 1-3	29.85	0.64	1.0
Al 1-4	39.79	0.48	1.2
Al 1-5	49.74	0.48	1.5
Al 1-6	59.69	0.48	1.7
Al 1-7	69.64	0.48	1.9
Al 1-8	79.59	0.48	2.2
Al 1-9	89.54	0.36	2.4
Al 1-10	99.49	0.42	2.7
Al 1-11	109.44	0.42	2.9
Al 1-12	119.39	0.42	3.2
Al 1-13	129.33	0.36	3.5
Al 1-14	139.28	0.36	3.8
Al 1-15	149.23	0.36	4.1

Other Data					
Bridgman (1937)					
Normal Pressure (kb)	10	20	30	40	50
Shear Strength (kb)	1.0	1.6	2.1	2.6	3.1

Table 9. Test Conditions for Magnesium

Magnesium 27°C			
Test Number	Normal Pressure (kb)	Total Revolutions (at 9.6 rph)	Shear Strength (kb)
Mgl-1	9.95	0.72	0.8
Mgl-2	19.90	0.88	1.0
Mgl-3	29.85	0.64	1.3
Mgl-4	39.79	0.56	1.6
Mgl-5	49.74	0.84	1.9
Mgl-6	59.69	0.96	2.0
Mgl-7	69.64	1.12	2.15
Mgl-8	79.59	1.36	2.3
Mgl-9	89.54	0.56	2.4
Mgl-10	99.49	0.48	2.5
Mgl-11	109.44	0.32	2.65
Mgl-12	119.39	0.56	2.8
Mgl-13	129.33	0.32	2.9
Mgl-14	139.28	0.56	3.0
Mgl-15	149.23	0.48	3.1

Other Data					
Bridgman (1937)					
Normal Pressure (kb)	10	20	30	40	50
Shear Strength (kb)	0.57	0.71	0.75	0.80	0.87
Vereshchagin (1960)					
Normal Pressure (kb)	25	50	100		
Shear Strength (kb)	2.8	6.44	15.12		

Table 10. Test Conditions for Bismuth

Tin 27°C			
Test Number	Normal Pressure (kb)	Total Revolutions (at 3.6 rph)	Shear Strength (kb)
Snl-1	9.95	0.62	0.4
Snl-2	19.90	0.62	0.5
Snl-3	29.85	0.62	0.6
Snl-4	39.79	0.62	0.75
Snl-5	49.74	0.48	0.9
Snl-6	59.69	0.48	1.0
Snl-7	69.64	0.48	1.1
Snl-8	79.59	0.48	1.25
Snl-9	89.54	0.32	1.4
Snl-10	99.49	0.32	1.5
Snl-11	109.44	0.40	1.65
Snl-12	119.39	0.48	1.80
Snl-14	129.33	0.32	1.9
Snl-15	139.28	0.32	2.1
Snl-16	149.23	0.32	2.2

Other Data					
Bridgman (1937)					
Normal Pressure (kb)	10	20	30	40	50
Shear Strength (kb)	0.28	0.41	0.80	0.71	0.77
Vereshchagin (1960)					
Normal Pressure (kb)	25	50	100	150	
Shear Strength (kb)	1.0	2.2	7.8	12.3	

Table 11. Test Conditions for Tin

Bismuth 27°C			
Test Number	Normal Pressure (kb)	Total Revolutions (at 9.6 rph)	Shear Strength (kb)
Bil-1	9.95	1.44	0.4
Bil-2	19.90	0.80	0.5
Bil-4	39.79	0.84	0.8
Bil-5	49.74	0.98	1.1
Bil-6	49.74	0.84	1.0
Bil-7	59.69	0.60	1.2
Bil-9	9.95	0.64	0.4
Bil-10	19.90	0.98	0.5
Bil-11	29.85	0.84	0.5
Bil-12	39.79	0.84	0.9
Bil-13	49.74	0.48	1.1
Bil-14	59.69	0.64	1.2
Bil-15	89.64	0.80	1.4
Pil-16	75.59	0.64	1.8
Bil-18	89.54	1.12	1.6
Bil-19	99.49	0.84	2.0
Bil-20	109.44	0.80	2.2
Bil-21	119.39	0.48	2.4
Bil-22	129.33	0.48	2.6
Bil-23	139.28	0.80	2.6
Bil-24	149.23	0.48	3.0

Other Data					
Bridgman (1937)					
Normal Pressure (kb)	10	20	30	40	50
Shear Strength (kb)	0.4	0.7	0.6	1.00	1.7
Vereshchagin (1960)					
Normal Pressure (kb)	25	50	100		
Shear Strength (kb)	1.05	2.31	3.15		

Three basic parameters characterize each curve: (1) the slope at low pressure between the sample andanvils, μ; (2) the slope at high pressures dS/dP which indicates the effect of pressure on strength; and (3) the intercept S_1 which indicates the shear strength of the grossly deformed materials at atmospheric pressure. Table 12 summarizes the experimental values of these parameters.

Table 12. Room Temperature Parameters

Element	Friction Coefficient	Strength Increase with Pressure dS/dP	Atmospheric Shear Strength S_1 (kb)
W	0.20	0.05	13.0
Ge	0.14	0.06	4.6
Ni	0.14	0.04	6.0
Be	0.17	0.02	7.1
U	0.20	0.02	9.7
Cu	0.11	0.01	3.2
Au	0.07	0.02	1.3
Ag	0.11	0.01	2.3
Al	0.02	0.02	0.4
Mg	0.02	0.01	1.3
Bi	0.01	0.01	0.1
Sn	0.01	0.01	0.1

The observed friction coefficients are of the order expected for slip of a hard metal on a softer metal in air where surface oxides and absorbed contaminant films may be present (Bowden and Tabor, 1964). Similar values were observed by Bridgman (1935, 1937) for many of the metals, and by Vereshchagin and Shapochkin (1960) for copper and silver.

The increase in strength with pressure, α, was observed in tensile tests in the range up to 30 kb by Bridgman (1952) on a variety of steels; the rate was typically 0.05. More recent tests by Pugh (1964) suggest that the rate is $\lesssim 0.02$ for O.F.H.C. copper and mild steel in the pressure range up to 4 kb. Bridgman's (1937) shear measurements on copper in the range from 40 to 50 kb indicate a rate $\lesssim 0.03$. Bridgman's value must be taken as an upper limit, because it is not clear that he went significantly beyond the transition knee of the torque-pressure curve.

Typical room-temperature values of S_1 deduced from tensile tests on grossly deformed copper, silver, and gold are 2.6 kb (99.4 percent), 1.7 kb (75 percent), and 1.1 kb (60 percent), respectively, where the numbers in parentheses indicate the percent reduction in area given the samples in prior coldworking (Metals Handbook, 1961). These values should be considered lower limits, since the present experiments were continued to larger strains (over 1000 percent) where workhardening ceased. A tensile test on commercial copper by Bridgman (1952)

suggests $S_1 \sim 3.0$ kb at a strain of 95 percent. Gross torsion experiments conducted by Crewe and Kappler (1964a, 1964b) on copper yield $S_1 \sim 2.7$ kb and exhibit qualitative features similar to the present investigations, although no high-pressure measurements were made.

Bridgman's (1937) shear measurements on metals such as nickel, uranium, silver, and gold, and those of Vereshchagin and Shapochkin (1960) on copper and silver show no knee in the shear strength versus pressure curves. Their high-pressure data fall on a continuation of the low-pressure slip curve. Such a result is explicable on the basis of an experimental technique that leads to anvil-to-anvil contact, as discussed previously.

Furthermore, through the use of Eq. (6) and typical values of the parameters S_1, μ, and α noted above, the knee should occur, for example, at pressures of 30, 20, and 15 kb for copper, silver, and gold, respectively. These are close to the locations in Figure 10 where the shear-strength normal-pressure curves for copper, silver, and gold are combined. Most of the following discussion will be based on the results of shearing copper, gold, and silver, inasmuch as most of the shear tests were performed on these elements and more published information in the literature exists for these metals.

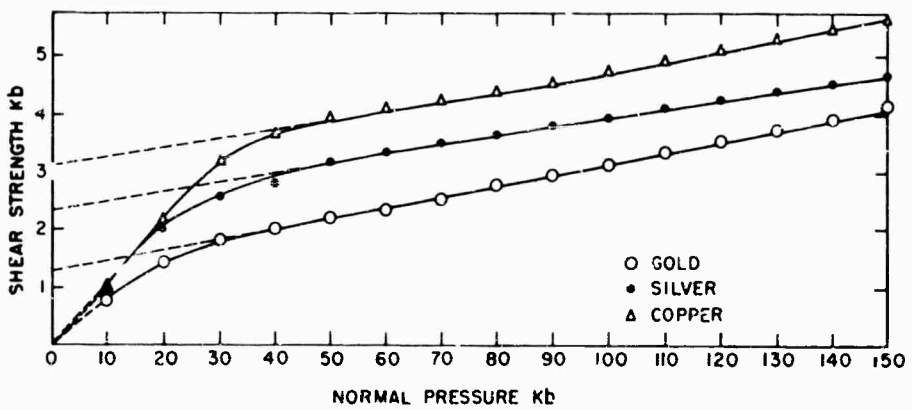

Figure 10. Observed Shear Curves of Copper, Silver, and Gold at 27°C. As explained in the text, the shear strength at pressures to the left of the knee in the curves must be obtained by extrapolation, as shown by the dashed lines

The above comparisons with independent experiments indicate the general validity of the data obtained by the present techniques and the theoretical model employed. Numerous additional measurements were made on copper, silver, and

gold at elevated temperatures and at various pressures. The results are summarized in Table 13. Data obtained below the threshold pressure, where restraining torque bears no immediate relationship to shear strength, were excluded to avoid misinterpretation. In all cases shear strength increases gradually with pressure at constant temperature, and decreases with rising temperature at constant pressure.

Table 13. Summary of Shear Strengths at Various Temperatures for Copper, Silver, and Gold

Table 13a. Copper

Temperature °C	Pressure (kb)	Shear Strength (kb)
27	0	3.2
27	0	3.7 *
27	50	3.9
27	50	4.2 *
27	60	4.1
27	70	4.2
27	80	4.4
27	90	4.5
27	100	4.7
27	110	4.9
27	120	5.1
27	130	5.3
27	140	5.4
27	150	5.7
230	50	2.8
300	0	1.8
300	40	2.2
300	50	2.3
300	50	2.5 *
400	50	1.6
400	50	1.5 *
500	0	0.5
500	20	0.75
500	30	0.8
500	40	0.9
500	50	1.0
500	50	1.0 *
700	50	0.7
700	50	0.6 *
900	0	0.25
900	20	0.25
900	30	0.25
900	40	0.25

*Sample given a preliminary work-hardening treatment.

Table 13b. Silver

Temperature °C	Pressure (kb)	Shear Strength (kb)
27	0	2.3
27	50	3.2
27	60	3.3
27	70	3.5
27	80	3.6
27	90	3.8
27	100	3.9
27	110	4.1
27	120	4.2
27	130	4.4
27	140	4.5
27	150	4.7
300	40	1.9
300	50	2.0
400	50	1.4
500	40	0.8
500	50	0.9
700	30	0.5
700	40	0.5

Table 13c. Gold

27	0	1.3
27	30	1.7
27	40	1.9
27	50	2.1
27	60	2.3
27	70	2.5
27	80	2.7
27	90	2.9
27	100	3.1
27	110	3.3
27	120	3.5
27	130	3.7
27	140	3.9
27	150	4.1
300	40	1.5
300	50	1.65
400	50	1.15
500	40	0.7
500	50	0.8
700	30	0.4
700	40	0.4

A series of tests were run on copper to determine the effect of previous work-hardening on shear strength. Samples were given a preliminary treatment by shearing them at 100 kb at room temperature, and then they were sheared at 50 kb at 27°C and at several higher temperatures. Data obtained on these treated samples are also shown in Table 13 and are marked with an asterisk. The data indicate that shear strength is nearly independent of the previous strain history under gross shear conditions.

The shear-strength data also were compared with an empirical formula recently suggested by Towle (1967), according to which the shear strength depends on temperature and pressure through the relation

$$S = S_o \exp\left[b \frac{T}{T_m(P)} \right] \tag{7}$$

where S_o and b are material parameters. Pressure enters this expression through its influence on the melting temperature, $T_m(P)$. Data from Table 13 are plotted on a semilogarithmic scale in Figure 11. The melting curves of Cohen et al. (1966) were used in the computations. Data obtained at pressures above 50 kb could not be used because of the limited pressure range of the available melting curves. Shear-strength values at atmospheric pressure were obtained by extrapolation, as shown in Figure 10. We omitted a few juxtaposed data points for clarity.

It is evident from Figure 11 that the data generally confirm Eq. (7). The shear strength of copper and silver are similar when compared at equivalent reduced temperatures, while gold is consistently weaker. Crosses represent data obtained on copper in gross torsion experiments by Grewe and Kappler (1964a, 1964b). Their data were obtained at atmospheric pressure in the temperature range 196°K to 800°K and they exhibit the same general trend as the present results. The measurements of Grewe and Kappler were made at a strain-rate two orders of magnitude lower than ours. This difference probably accounts for most of the numerical discrepancy indicated in Figure 11.

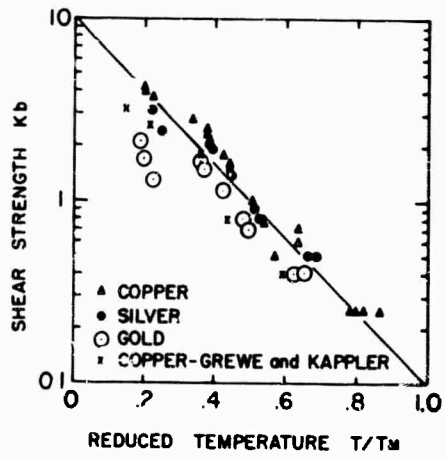

Figure 11. Shear Strength vs Reduced Temperature Plot of Gold, Silver, and Copper. These data from Table 13 were plotted on a semilogarithmic scale to test the empirical equation discussed in the text

All the data shown cluster about a straight line with an intercept, $S_o \sim 10$ kb, and a slope, $b \sim -5$. This intercept compares with the theoretical strength estimated for these materials at 0° K (NAS-NRC, 1966), and the slope compares with that observed with the face-centered-cubic materials argon, krypton, and silver chloride (Towle, 1967).

Equations (4) and (7) above are not independent. As an approximation the former may be derived from the latter when the melting temperature varies linearly at a slow rate with pressure. Then

$$T_m = T_{mo}(1 + \beta P) \tag{8}$$

where T_{mo} is the melting temperature at atmospheric pressure and β is a small constant. Equation (7) then becomes

$$S \sim S_o \exp\left[\frac{bT}{T_{mo}}\right]\left(1 - \frac{bT}{T_{mo}}\beta P\right). \tag{9}$$

Neither the exponential in Eq. (7) nor in Eq. (9) may be expanded directly because $bT/T_{mo} \sim 1$. Equation (9) compares with Eq. (4) with

$$S \equiv S_o \exp\frac{bT}{T_{mo}},$$

and

$$\alpha \equiv \frac{-bT}{T_{mo}}\beta S_1 .$$

When T_{mo} and β are given for a particular material, the constants b and S_o are determined from an isothermal shearing experiment in which the pressure is varied. An approximate shear strength could be computed at other temperatures and pressures through the use of Eq. (7). The expansion of the exponential required to obtain Eq. (9) is accurate within about 10 percent for $T/T_{mo} \lesssim 0.5$ for the three metals investigated. The usefulness of this technique is very limited, however, because Eq. (8) often is not valid over a wide pressure range. We consider Eq. (7) the more fundamental relationship, since it holds under conditions where the approximations leading to Eq. (9) are invalid.

An X-ray pattern of each element was also obtained on a General Electric diffractometer using Ni-filtered copper radiation before and after gross shear in an attempt to discover whether pressure or shear had induced any irreversible

polymorphic transitions. None was observed. The shear-strength normal-pressure curves also were examined for evidence of polymorphism. Bismuth exhibits a discontinuity in the shear curve between 20 and 30 kb normal pressure, which undoubtedly reflects the Bi I-II and Bi II-III transitions. The tests were not sensitive enough to define the precise location of the transformations in bismuth. In addition, several other known transitions were not detected by either technique. The discontinuous change in slope exhibited by the magnesium data is probably indicative of a polymorphic transition analogous to those reported by Bridgman (1935, 1937) in cadmium and zinc. We intend to pursue this question further.

X-ray analysis does reflect grain comminution and strain through line broadening in diffractograms.

Shear tests were also performed on germanium to investigate the strength behavior of an element whose melting point decreases with pressure. The melting point of germanium drops from 937°C at atmospheric pressure to 360°C at 180 kb. Figure 12 shows the resulting shear-strength normal-pressure curve for Ge, and the test conditions are given in Table 14. Figure 12 indicates that shear strength does not decrease with pressure as might be expected.

Table 14. Test Conditions for Germanium

Germanium 27°C			
Test Number	Normal Pressure (kb)	Total Revolutions (at 9.5 rph)	Shear Strength (kb)
Gel-4	9.95	0.64	1.4
Gel-5	19.90	0.64	2.8
Gel-6	29.85	0.64	4.4
Gel-7	39.79	0.40	5.8
Gel-8	49.74	0.40	7.3
Gel-9	59.69	0.40	8.1
Gel-10	69.64	0.40	8.6
Gel-11	79.59	0.40	9.2
Gel-12	89.54	0.48	9.7
Gel-13	99.49	0.40	10.4
Gel-14	109.44	0.48	10.9
Gel-15	119.39	0.32	11.5

Other Data					
Bridgman (1937)					
Normal Pressure (kb)	10	20	30	40	50
Shear Strength (kb)	1.4	2.7	3.9	4.9	5.7
Vereshchagin (1960)					
Normal Pressure (kb)	25	50	100	150	
Shear Strength (kb)	1.2	2.04	3.72	5.28	

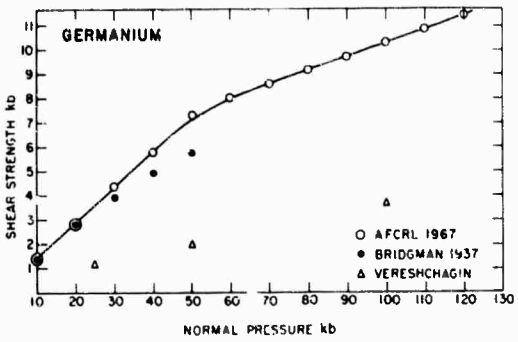

Figure 12. Shear Curve for Germanium at 27°C and a Strain Rate of 10^{-1}sec^{-1}. Test conditions given in Table 14

5. CONCLUSIONS

Table 15 summarizes the physical and observed mechanical properties for the 12 sheared elements. Note the excellent correlation between shear strength determined at 100 kb and microhardness. The correlation of strength with melting point is not as good. The high strength of uranium is accounted for in part by the presence of oxide contaminants, determined by X-ray.

Table 15. Summary of Physical and Mechanical Properties for Twelve Elements

Element	Packing or Crystal System	Melting Point at 1 bar	Diamond Pyramid Microhardness*	Shear Strength (kb) at Various Pressures			Rank of Melting Point	Rank of Hardness	Rank of Shear Strength	Element
				50 kb	100 kb	140 kb				
W	BCC	3410	1838	12.1	17.4	---	1	1	1	W
U	ORTHO	1132.3	282	10.4	12.0	13.9	4	3	2	U
Ge	DIA.CUBIC	937.4	864	7.3	10.4	---	8	2	3	Ge
Ni	FCC	1453	184.2	7.4	9.8	11.3	2	4	4	Ni
Be	HCP	1278	163.7	7.5	8.8	9.6	3	5	5	Be
Cu	FCC	1083	83.7	3.9	4.7	5.4	5	8	5	Cu
Ag	FCC	960.8	47.8	3.2	3.9	4.5	7	8	7	Ag
Au	FCC	1063	58.9	2.1	3.1	3.9	6	7	8	Au
Al	FCC	660.2	22.9	1.5	2.7	3.8	9	10	9	Al
Mg	HCP	651	31	1.9	2.5	3.0	10	9	10	Mg
Bi	RHOMB	271.3	9.2	1.1	2.0	2.8	11	11	11	Bi
Sn	TETRAG	231.9	8.7	0.9	1.5	2.1	12	12	12	Sn

*Measured using 136° diamond pyramidal indenter.

The studies have shown that an opposed anvil apparatus may be used to determine shear strength of elements at very high normal pressures. However, special care must be taken to insure that strength values are taken only beyond the surficial-slip regime, which may extend to very high pressures for strong materials. Low-pressure strength values may be estimated by extending the high-pressure slope of the shear-strength normal-pressure curve to intersect the ordinate. Unless care

is taken to prevent anvil-anvil contact during a shear test, the results will show erroneously high values for strength. The use of fresh samples for each test at pressure, and short shearing durations prevent the latter problem.

The shear data agree with independent strength measurements at low pressures, but differ significantly from high-pressure measurements by other investigators. We conclude that the divergence at high pressures may be explained by differences in experimental technique which lead to anvil contact.

The shear data for three metals—gold, copper, and silver, also fit a simple empirical formula relating the temperature and pressure dependence of shear strength.

Acknowledgments

This work was supported by the Advanced Research Projects Agency under ARPA Project 8671. We are grateful to Dr. Haskell of AFCRL and to M. Wilkens, D. Stevens, and A. Abey of Lawrence Radiation Laboratory for extensive technical assistance. All samples and the metallographic photos of copper were provided by Lawrence Radiation Laboratory.

References

Bowden, F. P., and Tabor, D. (1964) The Friction and Lubrication of Solids, Clarendon Press, Oxford, p. 564.

Bridgman, P. W. (1935) Effects of high shearing stress combined with high hydrostatic pressure, Rev. Rev. 48: 825-847.

Bridgman, P. W. (1937) Shearing phenomena at high pressures, particularly in inorganic compounds, Proc. Amer. Acad. Arts & Sci. 71: 387-460.

Bridgman, P. W. (1952) Studies in Large Plastic Flow and Fracture, McGraw-Hill, New York, p. 362.

Cohen, L. H., Kement, W., Jr., and Kennedy, G. C. (1966) Melting of copper, silver, and gold at high pressures, Phys. Rev. 145: 519-525.

Grewe, H. G., and Kappler, E. (1964a) Uber die ermittlung der verfestigungskurve durch den torsionsversuch an zylindrischen vollstaben und das verhalten von vielkristallinem kupfer bei sehr hoher plastischer schubverforming, Phys. Stat. Sol. 6: 339-354.

Grewe, H. G., and Kappler, E. (1964b) Strukturanderungen von vielkristallinem kupfer nach extrem hoher plastischer verformung, Phys. Stat. Sol. 6: 699-712.

Metals Handbook (1961) 8th Ed., V. i, American Society for Metals, Metals Park, Ohio, p. 1300.

Pugh, H. Ll. D. (1964) The Mechanical Properties and Deformation Characteristics of Metals and Alloys Under Pressure, Natl. Eng. Lab. Rpt. No. 142, p. 83.

Riecker, R. E. (1964a) New shear apparatus for temperatures of 1000°C and pressures of 50 kbars, Rev. Sci. Instru. 35: 596-598.

Riecker, R. E. (1964b) Use of induction heating in rock deformation apparatus, Rev. Sci. Instru. 35: 1234-1236.

Riecker, R. E., and Rooney, T. P. (1966a) Weakening of dunite by serpentine dehydration, Science 152: 196-198.

References

Riecker, R.E., and Rooney, T.P. (1966b) Shear Strength, Polymorphism, and Mechanical Behavior of Olivine, Enstatite, Diopside, Labradorite, and Pyrope Garnet: Tests to 920°C and 60 Kbar, Air Force Camb. Res. Labs. Rpt. AFCRL-66-543, p. 57.

Theoretical Strength of Materials (1966) Publication MAB-221-M of the Natl. Acad. Sci. - Natl. Res. Coun., Washington, D.C., p. 112.

Towle, L.C. (1967) Empirical relationship between shear strength, pressure, and temperature, App. Phys. Letters 10: 317-318.

Towle, L.C., and Riecker, R.E. (1966) Some consequences of pressure gradients in Bridgman anvil devices, J. Geophys. Res. 71: 2609-2618.

Vereshchagin, L.F., and Shapochkin, V.A. (1960) The effect of hydrostatic pressure on resistance to shear in solids, Fiz. Metal. Metalloved 9:258-264.

Vereshchagin, L.F., Zubova, E.V., and Shapochkin, V.A. (1960) Apparatus and methods of high pressure measurement of shear in solid bodies, Prib. i Teck. Eksper. (No. 5):89-93.

Unclassified
Security Classification

DOCUMENT CONTROL DATA - R&D

(Security classification of title, body of abstract and indexing annotation must be entered when the overall report is classified)

1. ORIGINATING ACTIVITY *(Corporate author)* Air Force Cambridge Research Laboratories (CRJ) L. G. Hanscom Field Bedford, Massachusetts 01730	2a. REPORT SECURITY CLASSIFICATION Unclassified 2b. GROUP

3. REPORT TITLE
SHEAR STRENGTH OF TWELVE GROSSLY DEFORMED METALS AT HIGH PRESSURES AND TEMPERATURES

4. DESCRIPTIVE NOTES *(Type of report and inclusive dates)*
Scientific. Interim.

5. AUTHOR(S) *(First name, middle initial, last name)*
R. E. Riecker
L. C. Towle
T. P. Rooney

6. REPORT DATE August 1967	7a. TOTAL NO. OF PAGES 31	7b. NO. OF REFS 18
8a. CONTRACT OR GRANT NO. ARPA Project 8671 b. PROJECT, TASK, WORK UNIT NOS. 7639-05-01 c. DOD ELEMENT 6240539F d. DOD SUBELEMENT 681000	9a. ORIGINATOR'S REPORT NUMBER(S) AFCRL-67-0475 9b. OTHER REPORT NO(S) *(Any other numbers that may be assigned this report)* ERP No. 273	

10. DISTRIBUTION STATEMENT
Distribution of this document is unlimited. It may be released to the Clearinghouse, Department of Commerce, for sale to the general public.

11. SUPPLEMENTARY NOTES This work was supported by the Advanced Research Projects Agency under ARPA Project 8671	12. SPONSORING MILITARY ACTIVITY Air Force Cambridge Research Laboratories (CRJ) L. G. Hanscom Field Bedford, Massachusetts 01730

13. ABSTRACT

The shear strength of grossly deformed tungsten, germanium, nickel, beryllium, uranium, copper, gold, silver, aluminum, magnesium, bismuth, and tin was measured in an opposed anvil shear apparatus at pressures up to 150 kb at 27°C, and for gold, silver, and copper to 900°C. The shear data agree with independent strength measurements at low pressures, but differ significantly from high-pressure shear-strength measurements made by other investigators. The data on the noble metals also fit a simple empirical formula relating the temperature and pressure dependence of the shear strength.

DD FORM 1 NOV 65 1473

Unclassified
Security Classification

14. KEY WORDS	LINK A		LINK B		LINK C	
	ROLE	WT	ROLE	WT	ROLE	WT
Shear Strength Metals Pressure Shear						